ELSEVIER

Surface Science 462 (2000) 19–35

surface science

www.elsevier.nl/locate/susc

Semi-empirical simulations of surface relaxation for perovskite titanates

E. Heifets [a], E.A. Kotomin [b,c,*], J. Maier [b]

[a] *Materials and Processes Simulation Center, Beckman Institute, Californian Technological Institute, Pasadena, CA 91125, USA*
[b] *Max-Planck-Institut für Festkörperforschung, Heisenbergstr., 1, Stuttgart 70569, Germany*
[c] *Institute of Solid State Physics, University of Latvia, 8 Kengaraga, Riga LV-1063, Latvia*

Received 31 March 2000; accepted for publication 16 May 2000

Abstract

The (100) and (110) surface relaxations are calculated for $SrTiO_3$ and $BaTiO_3$ perovskite thin films. By means of a semi-empirical shell model, the positions of atoms in 16 near-surface layers placed atop a slab of rigid ions are calculated. Surface rumpling and surface-induced dipole moments are calculated for all possible surface terminations. Our results for the (100) surface structure are in good agreement with ab-initio plane-wave pseudopotential calculations and LEED experiments. The surface energy for the Ba-, Sr-, TiO-terminated (110) surfaces is found to be much larger than that for the (100) surface. In contrast, the surface energy for the asymmetric O termination, where outermost O atoms are strongly on-plane-displaced, is the lowest for all (110) terminations and thus the most stable.

Keywords: Atomistic dynamics; Single crystal surfaces; Surface relaxation and reconstruction; Surface structure, morphology, roughness, and topography

1. Introduction

ABO_3 perovskite ferroelectric films are important for many applications including high-capacity memory cells, catalysis, optical waveguides, integrated optics applications, substrates for high-T_c cuprate superconductor growth, etc. [1–5]. In all cases, surface structure and quality are of primary importance. In this paper, we calculate the atomic structure of the $SrTiO_3$ and $BaTiO_3$ (100) and (110) surfaces in a cubic (paraelectric) phase of crystals. It should be noted that at all temperatures, bulk $SrTiO_3$ exhibits paraelectric properties, despite the antiferrodistortive (AFD) transition at 105 K to a tetragonal phase in which the oxygen octahedra have rotated in opposite directions in neighboring unit cells [6]. In contrast, iso-structural $BaTiO_3$ undergoes several phase transitions from paraelectric to ferroelectric phases as the temperature decreases.

The $SrTiO_3$ (100) surface has been relatively well studied. Its relaxation has been quantitatively characterized by means of low-energy electron diffraction (LEED), reflection high-energy electron diffraction (RHEED), and medium-energy ion scattering (MEIS) measurements [7–11]. Recently, several ab-initio studies (plane waves with pseudopotentials and Hartree–Fock formalism) were published for the (100) surface of $BaTiO_3$ and $SrTiO_3$ crystals, in which a few

* Corresponding author. Fax: +49-711-6891722.
E-mail address: kotomin@chemix.mpi-stuttgart.mpg.de (E.A. Kotomin)

0039-6028/00/$ - see front matter
PII: S0039-6028(00)00603-8

near-surface planes were allowed to relax [12–15] (see also Ref. [16] dealing with surface dynamic charges and polarization of $BaTiO_3$ (100) surface and semi-empirical estimates [17]). Owing to the large number of atomic coordinates to be optimized, such calculations are very complicated and time-consuming. An alternative approach is to use a classical *shell model* (SM) [18,19]. This semi-empirical approach has been used very successfully for many years for defect calculations in perovskite bulk crystals [18–25]. The great advantage of the SM is that it is well suited for the treatment of *polarization effects*, which are important for our study. Several SM studies dealt with $SrTiO_3$ (100) surfaces: Ref. [26] focused on the possible ferroelectric on-plane surface reconstruction, whereas the relaxation of several near-surface planes has been simulated in Ref. [27]. Here, we perform much more detailed SM studies for the two crystals with different terminations, allowing atomic relaxation of 16 near-surface planes.

The (110) surface has been less studied, but recently, it became a subject of intensive experimental investigations, focusing mainly on $SrTiO_3$, and using STM, UPS, and XPS spectroscopies [28,29] as well as Auger spectroscopy and LEED [30–34]. The atomic and electronic structure of the (110) surface were found to be strongly dependent on the annealing temperature. We are aware of the only theoretical calculation for the $SrTiO_3$ (110) surfaces [35]. This pilot study is based on the semi-empirical quantum chemical CNDO method and focused mainly on the surface effects on the electronic structure and surface density of states.

In this paper, we study an idealized case of perfect and flat surfaces, neglecting any possible complicated reconstructions, steps, etc. In particular, we focus on the surface rumpling since this is known to be quite considerable in many oxide crystals. We compare our calculations, whenever available, with electron diffraction experiments on the surface relaxation and ab-initio studies.

2. Method

In the present study, we have studied a periodic two-dimensional slab of cubic $SrTiO_3$ and $BaTiO_3$ crystals. To study the surface relaxation, we have optimized the atomic positions in several (varied from one to 16) near-surface planes, placed into the electrostatic field of the slab (simulated by 20 additional planes whose atoms were fixed in their perfect lattice sites). The number of these additional planes was chosen to reach a convergency of the crystalline field in the surface planes.

In the SM, the interatomic interactions are described by the core–core, core–shell and shell–shell pair potentials. In this approach, each ion has a charged core and an electronic shell. The sum of the core and shell charges is equal to the formal charge of the corresponding ion. The spring constant, k, connects the core and the shell of the same ion. The core–shell separation is a measure of the *atom polarization*. The interactions between the cores and between cores and shells of different ions are Coulombic, whereas the interactions between the shells of different ions besides the Coulombic part also contain the short-range potentials accounting for the effects of the exchange repulsion together with the van der Waals attraction between them. The short-range Buckingham potentials contain three parameters, A, ρ, and C per pair of atoms. All parameters for $BaTiO_3$ and $SrTiO_3$ were carefully fitted to the lattice structure, elastic and dielectric properties of crystals (see details in Refs. [20–22]). Say, for the $SrTiO_3$ the calculated elastic constants are: $c_{11}=30.15$ (33.0), $c_{12}=13.74$ (10.10), $c_{44}=13.78$ (12.40) (in units of 10^{11} dyne/cm^2). These values are in good agreement with the relevant experimental values given in brackets and give confidence to the use of SM for the surface relaxation study. The agreement of theoretical values for low-/high-frequency dielectric constants carried out in the framework of the used pair potentials with the experimental results supports the SM applicability in perovskite studies. The pair potentials [20–25] were successfully used in the relevant defect calculations in the perovskite bulk. Lastly, the good quality of these potentials also follows from the agreement between calculated and experimental phonon frequencies for $SrTiO_3$ (in units of 10^{12} s^{-1}): 8.50 (7.95) at the Γ_{25} point of the BZ and 13.03 (13.40) at R_{12} (experimental values [36] are given in brackets). Detailed SM calculations of phonon frequences in $SrTiO_3$ were presented recently in Ref. [37].

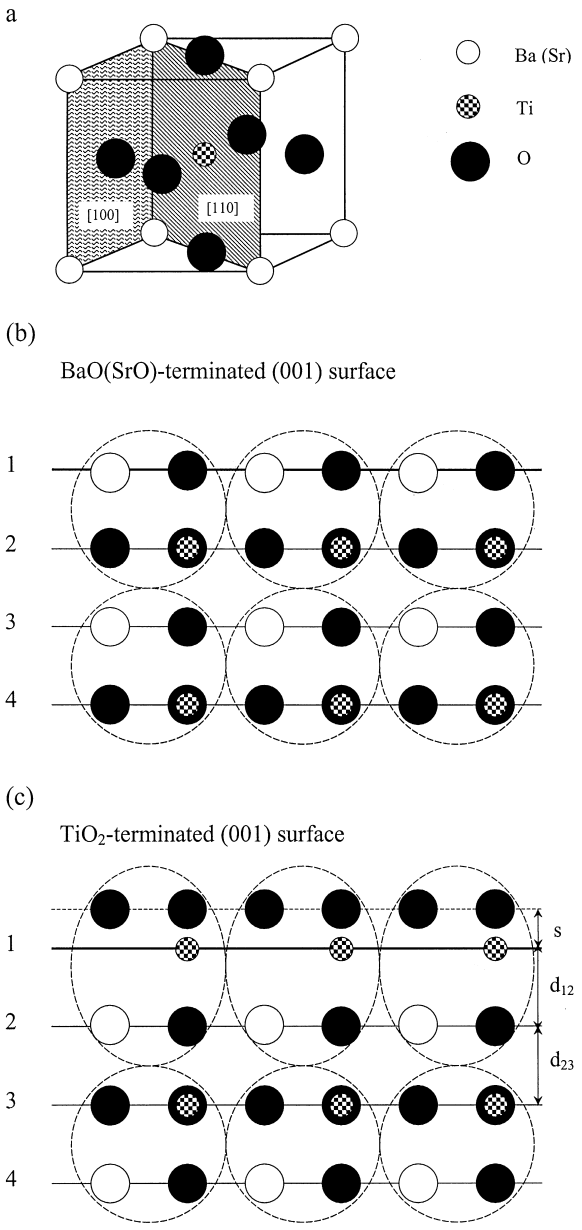

Fig. 1. (a) Sketch of the cubic perovskite structure with shaded (100) and (110) surfaces. (b, c) Side view of BaO(SrO)- and TiO_2-terminated (100) surfaces with the definitions of the surface rumpling s and the near-surface interplane distances, d_{12} and d_{23}, respectively.

Note that the use of integer ionic charges does not imply restrictions of the SM to purely ionic materials; in fact, the short-range potential effectively takes into account the covalency and charge-transfer effects. Atomistic surface relaxation is found by means of the MARVIN computer code [38]. This code is based on the shell-model technique suited for simulations of surface structures.

In our slab calculations, we simulated Ti- and Sr(Ba)-terminated (100) surfaces as well as Ba-, Ti- and O-terminated (110) surfaces. The (100) surface is neutral and very simple. Fig. 1 shows a view of the (100) surface and the sequence of near-surface planes for the two above-mentioned terminations. For the Ti termination, O atoms can be displaced with respect to 'their' Ti atoms belonging to the same plane, by the quantity, s, called the surface rumpling. Atomic displacements from ideal planes also change distances between several near-surface planes as compared to those in a perfect crystal. The quantities s, d_{12}, and d_{23} shown in Fig. 1c are measured experimentally, e.g. by means of LEED or RHEED. Our calculations of the interplane distances are based on the metal ion (Ti or Sr) displacements from unrelaxed planes, which are known to be much stronger electron scatterers than O ions [7]. (Note that in some studies, e.g. Ref. [14], d_{12}-type quantities are calculated as average metal and O displacements from the same plane.) In SM calculations, atoms from one to 16 near-surface planes were allowed to relax in order to achieve the minimum of total energy. As a result, we obtain the optimized slab geometry and dipole moments caused by core and electron shell displacements from regular lattice sites. The surface energy was calculated as $E_s = E_{tot} - E_1 - nE_{bulk}$, where E_{tot} is the total energy for a slab of n relaxed planes placed on the rigid substrate, E_{bulk} is the total energy per bulk unit cell, and E_1 is the interaction energy between the relaxed slab and the rigid substrate. Note that the SM was applied by us very recently in preliminary calculations of (100) surface relaxations for $BaTiO_3$ [39] and $SrTiO_3$ [40,41].

3. Main results

3.1. (100) surfaces

Tables 1 and 2 list the displacement magnitudes for atomic cores and shells for four top layers near

Table 1
Relaxation of the uppermost four layers in the Sr- and Ti-terminated $SrTiO_3$ (100) surfaces[a]

Sr-terminated				Ti-terminated			
Layer number	Ion	Type	Δz (%)	Layer number	Ion	Type	Δz (%)
1	Sr^{2+}	Core	−7.10 (−5.7)	1	Ti^{4+}	Core	−2.96 (−3.4)
		Shell	−5.03			Shell	−2.88
	O^{2-}	Core	1.15 (0.1)		O^{2-}	Core	−1.73 (−1.6)
		Shell	−3.15			Shell	−2.40
2	Ti^{4+}	Core	1.57 (1.2)	2	Sr^{2+}	Core	3.46 (2.5)
		Shell	1.53			Shell	2.63
	O^{2-}	Core	0.87 (0.0)		O^{2-}	Core	−0.21 (−0.5)
		Shell	1.21			Shell	1.34
3	Sr^{2+}	Core	−1.42 (−1.2)	3	Ti^{4+}	Core	−0.60 (−0.7)
		Shell	−1.10			Shell	−0.59
	O^{2-}	Core	0.70 (−0.1)		O^{2-}	Core	−0.29 (−0.5)
		Shell	−0.58			Shell	−0.43
4	Ti^{4+}	Core	0.19	4	Sr^{2+}	Core	0.49
		Shell	0.18			Shell	0.37
	O^{2-}	Core	0.04		O^{2-}	Core	−0.10
		Shell	0.10			Shell	0.14

[a] In total, 16 near-surface planes were allowed to relax. Ionic displacements are expressed as a percentage of $a_0 = 3.8969$ Å (the bulk crystal lattice parameter). Positive (negative) displacements mean the direction outwards (inwards) the surface. Numbers in brackets are the results of ab-initio calculations [12].

Table 2
Relaxation of the uppermost four layers in the Ba- and Ti-terminated $BaTiO_3$ (100) surfaces ($a_0 = 3.9596$ Å)[a]

Ba-terminated				Ti-terminated			
Layer number	Ion	Type	Δz (%)	Layer number	Ion	Type	Δz (%)
1	Ba^{2+}	Core	−3.72 (−2.79)	1	Ti^{4+}	Core	−2.72 (−3.89)
		Shell	−3.43			Shell	−2.66
	O^{2-}	Core	1.00 (−1.4)		O^{2-}	Core	−0.94 (−1.63)
		Shell	−2.76			Shell	−1.75
2	Ti^{4+}	Core	1.25 (0.92)	2	Ba^{2+}	Core	2.19 (1.31)
		Shell	1.23			Shell	2.09
	O^{2-}	Core	0.76 (0.48)		O^{2-}	Core	−0.17 (−0.62)
		Shell	1.03			Shell	1.04
3	Ba^{2+}	Core	−0.51 (−0.53)	3	Ti^{4+}	Core	−0.33 (−0.75)
		Shell	−0.48			Shell	−0.32
	O^{2-}	Core	0.16 (−0.26)		O^{2-}	Core	−0.01 (−0.35)
		Shell	−0.26			Shell	−0.14
4	Ti^{4+}	Core	0.20	4	Ba^{2+}	Core	0.39
		Shell	0.19			Shell	0.31
	O^{2-}	Core	0.11		O^{2-}	Core	−0.02
		Shell	0.15			Shell	0.16

[a] Numbers in brackets are the results of ab-initio calculations [13].

the surface. Our calculations show that Ti^{4+}, Ba^{2+} (Sr^{2+}), and O^{2-} ions in the planes close to the surface reveal very different displacements from their perfect crystalline sites. One can also see the difference between the BaO(SrO)- and TiO_2-terminated surfaces. In most cases, the surface ions are

displaced inwards, whereas the ionic displacements in the second layer point outwards from the crystal. In particular, on the SrO-terminated surface of $SrTiO_3$, the surface ions shift inwards by 7% of the bulk lattice constant ($a_0 = 3.89$ Å), whereas in the third layer, the displacements of Sr ions are reduced to 1.4%. Similarly, on the BaO-terminated surface of $BaTiO_3$, the surface ions shift inward by 3.7% of bulk lattice constant ($a_0 = 3.96$ Å) and by 0.5% in the third layer. Ti ions are displaced outwards the $SrTiO_3$ crystal by $\approx 1.6\%$ in the second layer. In $BaTiO_3$ this value is $\approx 1.3\%$, and inward displacement of Ti in the fourth layer in both crystals is $\approx 0.2\%$. The cores of O ions in the first plane in both crystals are displaced outward, but their shells are displaced inwards, which means strong O atom polarization. In turn, *both* O cores and shells relax outwards on the Ti-terminated surface. The magnitudes of ionic displacements fall down essentially for the deeper layers, except for the Sr ions in the third layer, which still exceeds 1%.

Very similar trends in ionic displacements are observed for the Ti-terminated surface (Table 1). The inward displacemens of the surface Ti ions are $\approx 3\%$ in $SrTiO_3$ ($\approx 2.7\%$ in $BaTiO_3$), and the outward displacements of Sr (Ba) ions in the second layer are nearly the same in magnitude. The O ions are displaced inwards in the top layer; again, we can see the opposite displacement directions for the O cores and shells in the second plane. The displacements of ions in deeper layers decrease approximately sixfold and practically vanish, starting with the five or six layers.

We performed calculations of the *surface energy*, E_s, for the relaxed surfaces. Its magnitude of the surface energy saturates when more than eight near-surface planes are allowed to relax (Figs. 2 and 3). In the case of the Ba-terminated $BaTiO_3$ surface, $E_s = 1.45$ eV/cell, which is only slightly larger than that for the Ti-terminated case (1.40 eV). This tiny difference appears to be entirely due to the difference in the relaxation energies of the surfaces in both cases. Since the difference is very small, both types of surfaces should co-exist, which is confirmed by both ab-initio calculations [6] and experiments [7]. For $SrTiO_3$, the Ti-terminated surface energy of

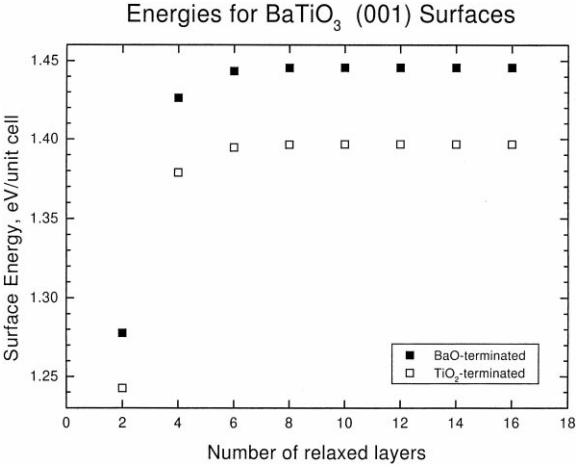

Fig. 2. Surface energies for $BaTiO_3$ (100) vs. the number of relaxed near-surface planes.

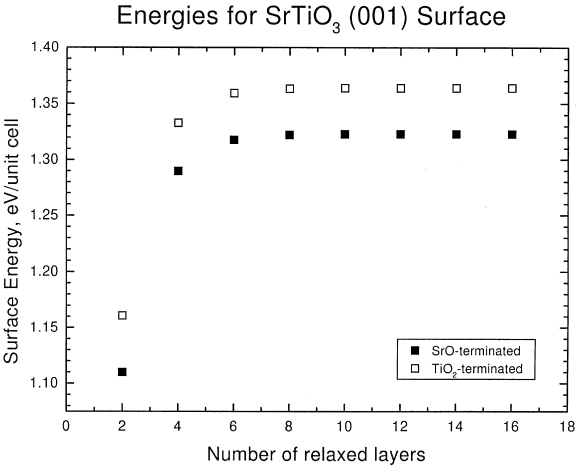

Fig. 3. Surface energies for $SrTiO_3$ (100) surfaces vs. the number of relaxed near-surface planes.

1.37 eV is slightly larger than that for Sr termination (1.33 eV/cell). The ab-initio calculations [12,13] gave quite similar average surface energies (1.26 and 1.24 eV/cell for $SrTiO_3$ and $BaTiO_3$, respectively).

Calculations of the surface dipole moments for different numbers of relaxed layers reveal *strong oscillations* as the number of relaxed near-surface layers increases from one to six (Figs. 4 and 5). For a larger number of relaxed layers, these oscillations practically vanish, and the dipole

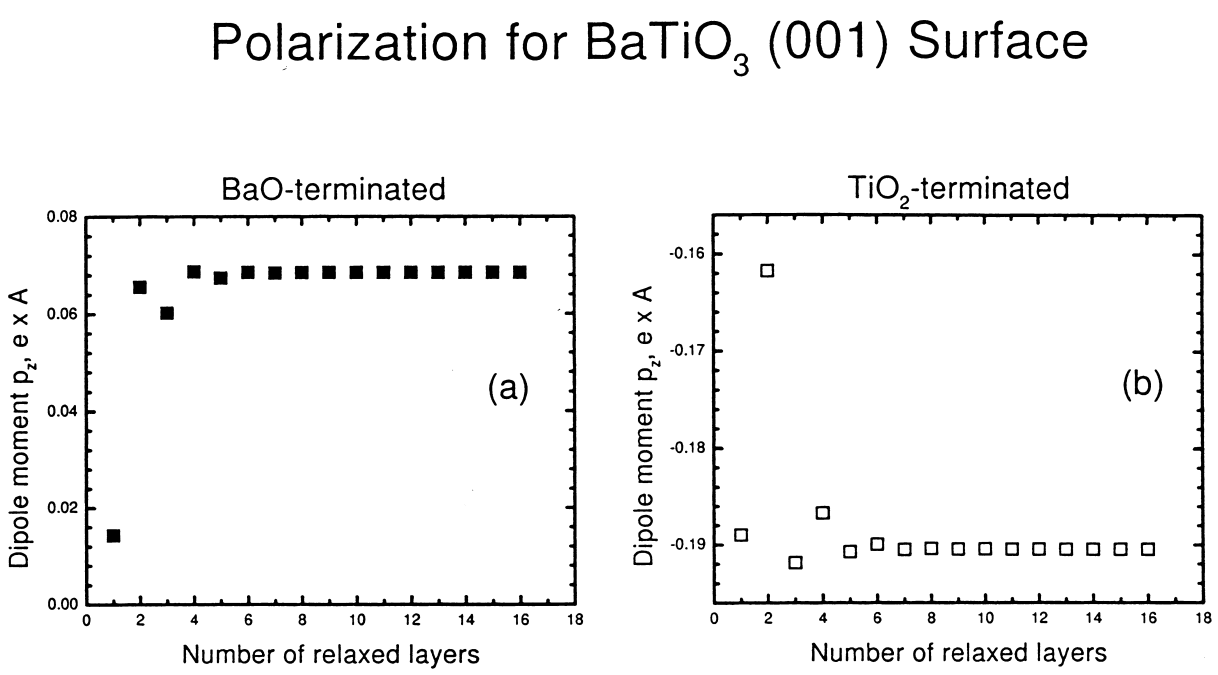

Fig. 4. Surface induced dipole moments for BaO- and TiO_2-terminated $BaTiO_3$ as a function of the number of near-surface planes allowed to relax.

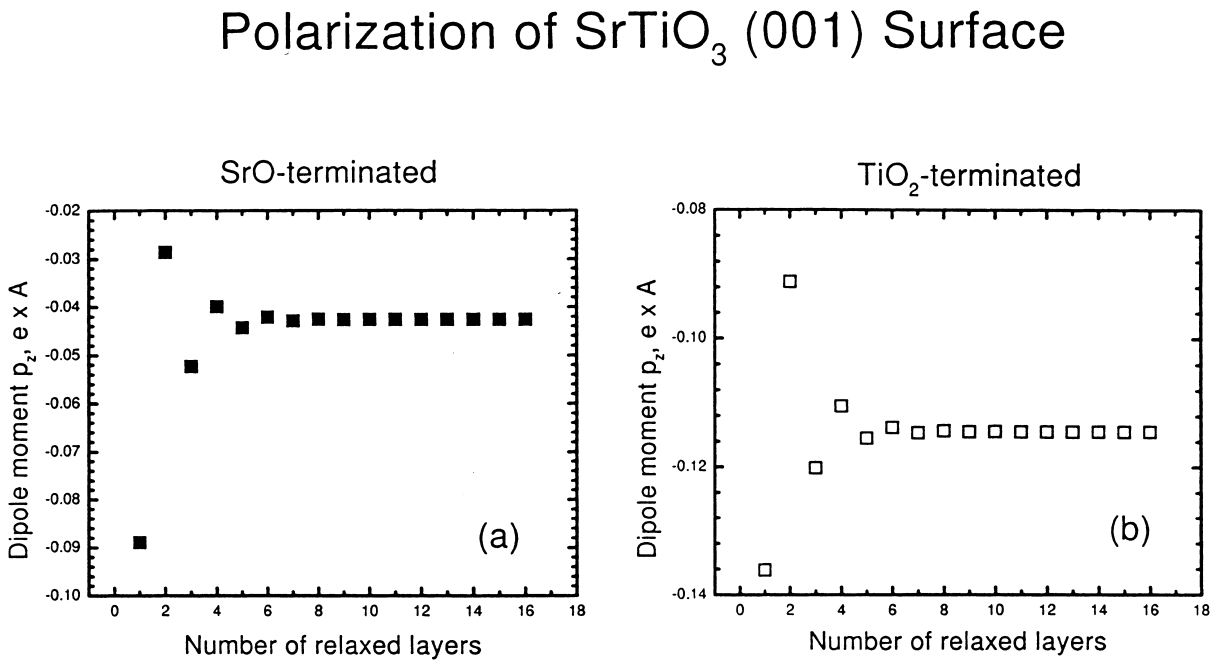

Fig. 5. Surface induced dipole moments for SrO- and TiO_2-terminated $SrTiO_3$ (001) as a function of the number of near-surface planes allowed to relax.

moments saturate at the level of 0.1–0.2 e · Å. Note that the same number of layers (six) was found by us to be necessary to reach convergency of the crystalline field in the surface region. These results show that the influence of the (100) surface extends down to five or six atomic layers inside the $BaTiO_3$ and $SrTiO_3$ crystals.

For both $SrTiO_3$ surfaces, the dipole moments are negative (Fig. 5), whereas for Ba termination, the dipole moments are positive (but close to zero; Fig. 4). For the Ti-terminated surfaces, the negative sign of the surface dipole moment comes from a larger inward displacement of Ti^{4+} ions, in comparison with those for the O^{2-} ions. The opposite direction of the displacement of Ba^{2+} or Sr^{2+} ions in the second layer only partly reduces the large dipole moment created by Ti displacements. For the Sr-terminated surface, the displacements of Sr ions are so large (7.1%) that the opposite displacements of Ti ions in the second layer cannot change the resulting sign of a surface dipole moment (but they do so for the Ba-terminated surface).

In all cases, a large *polarization* of ions in the near-surface layers takes place; it manifests itself through the large difference in displacements of cores and shells of the same ions. These differences for Ti ions sometimes appear quite small, but recall that the effective charge of Ti shell is very large, 35.86 e. This leads to the large dipole moment of Ti ions, even for the relatively small relative core–shell shifts. The observed large polarization of the ions indicates the appearance of a significant *electric field* near the surfaces of these paraelectric crystals.

A comparison of our calculations with the ab-initio plane-wave studies is presented in Table 3. The agreement is very good in all cases. (Recent Hartree–Fock (HF) calculations [15] for the Ba-terminated $BaTiO_3$ are only in qualitative agreement with plane-wave results and our SM findings. This could be caused by the limited basis set and different treatment of very localized *d* electrons in the plane-wave pseudopotential and HF approaches.) Also, we observe only a qualitative agreement with the previous SM calculations for $SrTiO_3$ [27] (Table 3). However, all theoretical methods give the same signs for both the rumpling and change in interplanar distances.

The results of the LEED and RHEED experiments [7–9] presented in Table 3 suggest relaxations quite different from calculated quantities. Note also that these two experiments contradict each other (e.g. in the sign of the d_{12} for Sr-terminated surface). Both our calculations and ab-initio plane wave calculations are closer to the experimental data [7]. Finally, it was found in recent MEIS experiments [10] for the Ti-terminated $SrTiO_3$ surface that $s \approx 2\%$, which is close to our result in Table 3. However, despite a good agreement for the O and Ti atom displacements from the top plane relative to each other, one serious question remains open: both experiments argue that the topmost O atoms move out from the surface, whereas all calculations indicate that in most cases, O moves in towards the surface.

3.2. (110) surfaces

The problem with modelling the (110) surfaces of $SrTiO_3$ and $BaTiO_3$ is that they consist of charged planes. In other words, if the (110) surface were to be modelled exactly as one would expect after crystal cleavage, it would have an infinite dipole moment perpendicular to the surface, which would make the surface unstable. To avoid this problem, in our calculations, we removed half the O atoms from the O-terminated surface, the Sr (Ba) atoms from the Ti-terminated surface, and the Ti and O atoms from the Sr(Ba)-terminated surface (Fig. 6). As a result, we obtain the so-called type-II stable surface with charged planes but a zero dipole moment [42]. The relevant surface cells are built from neutral five-atom elements from three successive planes, which are shown as encircled dashed ellipses in Fig. 6.

The initial atomic configuration for the O-terminated surface, where every second surface O atom is removed and others occupy the same sites as in the bulk structure, is termed hereafter asymmetric, denoted in the tables as *A*. Since such a removal of half of O atoms disturbs the balance of interatomic forces along the surface, we also studied another, symmetric initial surface configuration (denoted as *B*) in which the O atom is

(a)

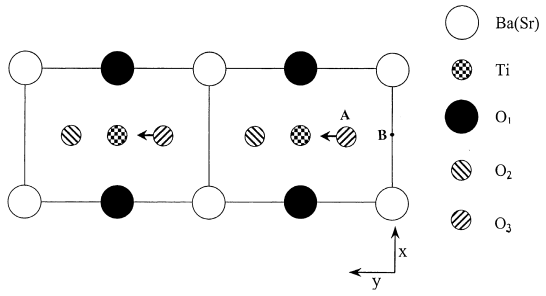

(b) O-terminated (011) surface, configuration **A** (initial guess)

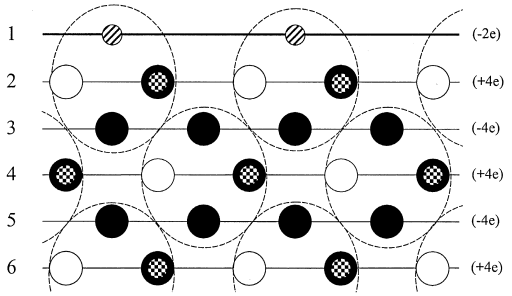

(c) O-terminated (011) surface, configuration **B** (initial guess)

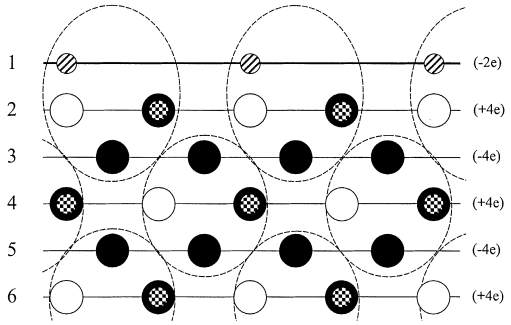

(d) O-terminated (011) surface, configuration **A** (relaxed)

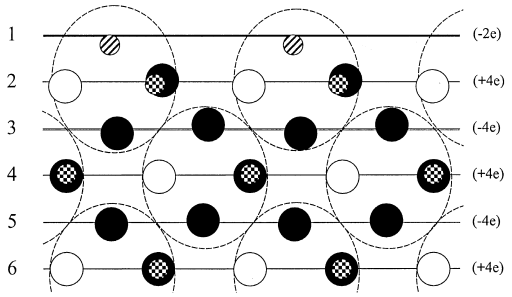

(e) O-terminated (011) surface, configuration **B** (relaxed)

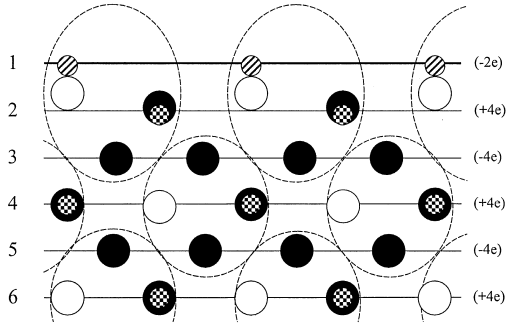

(f) TiO-terminated (011) surface (relaxed)

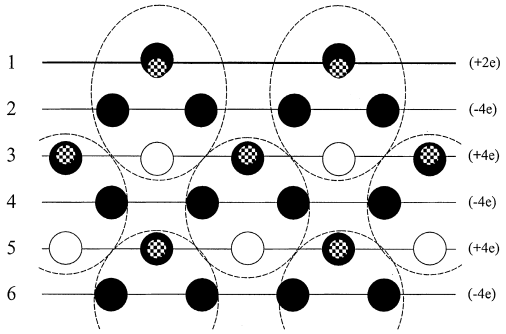

(g) Ba-terminated (011) surface (relaxed)

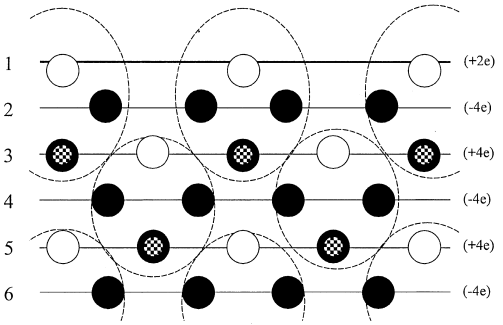

Table 3
Surface rumpling, s, and relative displacements of the three near-surface planes (see Fig. 1c for explanations) for the Sr(Ba) and Ti-terminated $SrTiO_3$ and $BaTiO_3$ (100) surfaces (as a percentage of the bulk lattice parameters)

$SrTiO_3$							
Sr-terminated				Ti-terminated			
Method	s	d_{12}	d_{23}	Method	s	d_{12}	d_{23}
Present study	8.2	−8.6	3.0	Present study	1.2	−6.4	4.0
Shell model [27]	4.5	−4.75	1.45	Shell model [27]	1.1	−3.95	1.2
Ab initio [12]	5.8	−6.9	2.4	Ab initio [12]	1.8	−7.0	3.2
LEED experiment [7]	4.1±2	−5±1	2±1	LEED experiment [7]	2.1±2	1±1	−1±1
RHEED experiment [8,9]	4.1	2.6	1.3	RHEED experiment [8,9]	2.6	1.8	1.3
$BaTiO_3$							
Sr-terminated				Ti-terminated			
Method	s	d_{12}	d_{23}	Method	s	d_{12}	d_{23}
Present study	2.7	−5.0	1.8	Present study	1.8	−4.9	2.5
Ab initio [13]	1.4	−3.7	1.5	Ab initio [13]	2.3	−5.2	2.0

placed in the middle of the distance between two equivalent O atoms in the bulk (cf. Fig. 6b and c). Some preliminary results were discussed in Ref. [43].

The calculated surface energies for $BaTiO_3$ and $SrTiO_3$ are shown in Figs. 7 and 8, which suggest several conclusions. First, the surface energies saturate quite fast as a function of the number of relaxed layers. Second, for Ba-, Sr-, Ti terminations, these energies are of the order of 2–4 eV/cell, e.g. much larger than those for the (001) surfaces. Third, the O-terminated asymmetric surfaces have considerably lower energies for both $BaTiO_3$ and $SrTiO_3$, these energies turn out to be close to those for the (100) surface. Thus, O termination should predominate when crystals are cleaved along the (110) plane or grown. (Oscillations in E_s for the $SrTiO_3$ surface will be discussed below.) This qualitative conclusion agrees well with recent CNDO

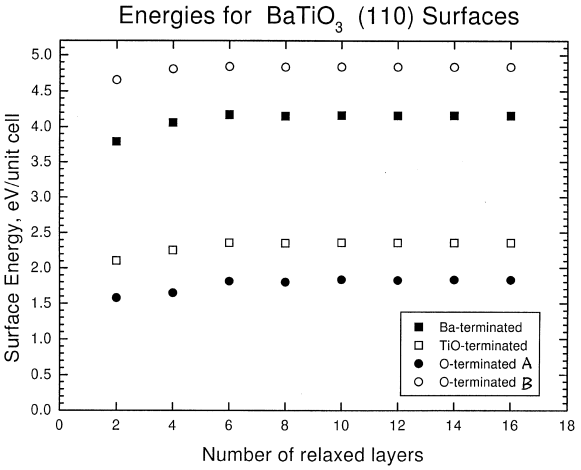

Fig. 7. Surface energies for $BaTiO_3$ (110) vs. the number of relaxed near-surface planes.

Fig. 6. (a) Top view of the (110) O-terminated surface, directions of the O atom displacements are shown by arrows. In our model, we remove atoms O_2 from the O-terminated surface and search for the atomic relaxations when O_3 are placed intially into asymmetric or symmetric positions A and B, respectively (see the text for explanations). Atoms of Ti, Ba(Sr) and O_1 lie in the second plane below the O-surface plane. (b, c) Side view of the two possible initial configurations A and B. (d, e) Relaxed A and B configurations. (f, g) Relaxed TiO- and Ba-terminated surfaces. Dashed ellipses containing five atoms in the three nearest planes show neutral fragments from which the surface unit cell is built. Numbers in brackets on the right-hand side indicate the corresponding effective charges of related planes in the cells.

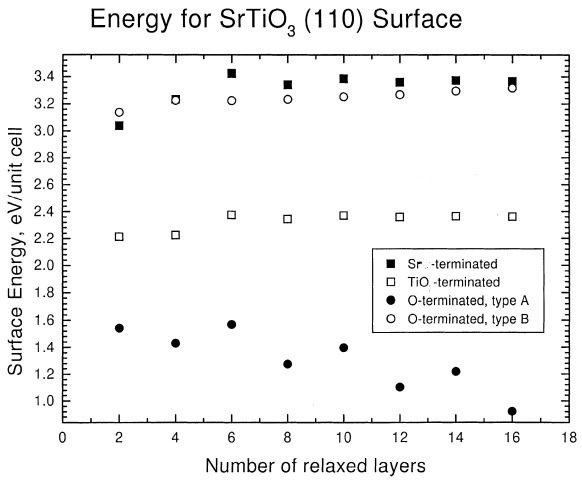

Fig. 8. Surface energies for $SrTiO_3$ (110) surfaces vs. the number of relaxed near-surface planes.

calculations [35] in which the O-terminated $SrTiO_3$ surface energy was found to be as low as 1.1 eV/cell. However, symmetrical O termination (Fig. 6c) is energetically costly and thus unfavourable.

Tables 4–7 for the (110) surfaces are similar to those for the (100) surfaces, whereas Table 8 complements these data by the predicted surface rumpling and the relative displacements of the two top layers. For the Ti-terminated surface, the rumpling for both $SrTiO_3$ and $BaTiO_3$ (110) surfaces is similar and very large, $\approx$13–14%. This arises due to a combination of a strong O ion outward displacement (6–8%) and Ti ion inward displacement (by 6%; see Tables 4 and 6). This relaxation is much larger than that found for the (100) surface. The reduction of relative distances between the first three layers is similar for both crystals, about 4–5%. Note, also, that surface ions are strongly polarized. For instance, the core–shell relative displacement for the Sr is 4.5%, and that for the O in the second plane of $SrTiO_3$ is 2.4%, etc.

For the O-terminated surface, when O ions are placed initially into symmetrical (*B*) surface positions, all near-surface atoms are displaced practically only along the *z*-axis perpendicular to the surface (Fig. 6c, e). During the relaxation, O atoms move slightly inwards, by $\approx$3% in both crystals (Tables 5 and 7). Ti ions in the second plane also do so, which results in a relatively small decrease in the d_{12} distance. This is, however, accompanied by a huge 27–30% outward displacement of Sr

Table 4
Relaxation of the uppermost four layers in the Sr- and Ti-terminated $SrTiO_3$ (110) surfaces (see Fig. 6f and g)

Sr-terminated				Ti-terminated			
Layer number	Ion	Type	Δz (%)	Layer number	Ion	Type	Δz (%)
1	Sr^{2+}	Core	−19.07	1	Ti^{4+}	Core	−5.99
		Shell	−14.54			Shell	−5.86
2	O^{2-}	Core	3.18		O^{2-}	Core	8.48
		Shell	0.79			Shell	6.62
3	Sr^{2+}	Core	4.67	2	O^{2-}	Core	−1.72
		Shell	5.04			Shell	−0.10
	O^{2-}	Core	−0.25	3	O^{2-}	Core	−4.10
		Shell	0.96			Shell	−3.82
	Ti^{4+}	Core	−0.89		Ti^{4+}	Core	2.14
		Shell	−0.92			Shell	2.16
4	O^{2-}	Core	0.42		Sr^{2+}	Core	−6.96
		Shell	0.30			Shell	−5.79
5	Ti^{4+}	Core	0.82	4	O^{2-}	Core	0.69
		Shell	0.81			Shell	0.67
	O^{2-}	Core	−1.44				
		Shell	−1.34				
	Sr^{2+}	Core	−3.27				
		Shell	−2.64				

Table 5
Relaxation of the uppermost four layers in the $SrTiO_3$ O-terminated (110) surfaces[a]

O-terminatedlayer number	Ion	Type	*A*		*B*
			Δy (%)	Δz (%)	Δz (%)
1	O^{2-}	Core	−8.54	−14.2	−2.78
		Shell	−8.34	−17.9	−3.17
2	Ti^{4+}	Core	−8.27	−2.37	−5.14
		Shell	−8.08	−2.36	−5.00
	Sr^{2+}	Core	−10.79	4.10	30.32
		Shell	−9.85	5.05	30.33
	O^{2-}	Core	8.20	5.71	9.68
		Shell	7.71	4.65	7.89
3	O^{2-}	Core	−11.01	−11.06	−2.41
		Shell	−8.51	−8.62	−0.51
4	Sr^{2+}	Core	−3.47	−4.86	−6.53
		Shell	−2.52	−4.26	−5.50
	Ti^{4+}	Core	1.82	1.99	2.38
		Shell	1.53	1.98	2.40
	O^{2-}	Core	−0.10	−0.10	−2.56
		Shell	0.0	0.0	−2.33

[a] *A* and *B* correspond to the asymmetric and symmetric starting O positions (see the text and Fig. 6a–c for explanations).

Table 6
Relaxation of the uppermost four layers in the Ba- and Ti-terminated $BaTiO_3$ (110) surfaces

Ba-terminated				Ti-terminated			
Layer number	Ion	Type	Δz (%)	Layer number	Ion	Type	Δz (%)
1	Ba^{2+}	Core	−13.49	1	Ti^{4+}	Core	−6.93
		Shell	−12.94			Shell	−6.80
2	O^{2-}	Core	2.80		O^{2-}	Core	6.45
		Shell	0.74			Shell	4.81
3	Ba^{2+}	Core	2.52	2	O^{2-}	Core	−1.66
		Shell	2.62			Shell	−0.10
	O^{2-}	Core	−2.94	3	O^{2-}	Core	−2.40
		Shell	−1.88			Shell	−2.31
	Ti^{4+}	Core	−1.20		Ti^{4+}	Core	1.59
		Shell	−1.21			Shell	1.61
4	O^{2-}	Core	0.33		Ba^{2+}	Core	−3.85
		Shell	0.24			Shell	−3.76
5	Ti^{4+}	Core	0.40	4	O^{2-}	Core	0.49
		Shell	0.39			Shell	0.67
	O^{2-}	Core	−0.19				
		Shell	−0.23				
	Ba^{2+}	Core	−1.00				
		Shell	−0.97				

(Ba) ions from the second plane. However, when O ions in $SrTiO_3$ and $BaTiO_3$ are placed initially in asymmetrical positions, *A* (Fig. 6b, d), atoms also reveal on-plane displacements, i.e. in the direction parallel to the surface. As a result, we found another optimized surface structure, with considerably less surface energy (Figs. 7 and 8). In this structure, Ba (Sr) atoms in the second plane are

Table 7
Relaxation of the uppermost four layers in the $BaTiO_3$ O-terminated (110) surfaces[a]

O-terminatedlayer number	Ion	Type	*A*		*B*
			Δy (%)	Δz (%)	Δz (%)
1	O^{2-}	Core	−6.70	−11.16	−2.89
		Shell	−2.58	−15.54	−3.80
2	Ti^{4+}	Core	−5.33	−1.83	−6.18
		Shell	−5.23	−1.83	−6.06
	Ba^{2+}	Core	−2.21	4.84	26.45
		Shell	−2.20	4.95	26.35
	O^{2-}	Core	5.90	4.54	5.89
		Shell	5.36	3.66	4.44
3	O^{2-}	Core	5.58	6.52	−2.30
		Shell	5.90	5.32	−0.68
4	Ba^{2+}	Core	0.65	−2.10	−3.70
		Shell	0.67	−2.00	−3.63
	Ti^{4+}	Core	−0.24	1.47	1.61
		Shell	−0.23	1.47	1.62
	O^{2-}	Core	0.50	0.85	−1.08
		Shell	0.36	0.79	−1.11

[a] *A* and *B* correspond to the asymmetric and symmetric starting O positions (see the text and Fig. 6a–c for explanations).

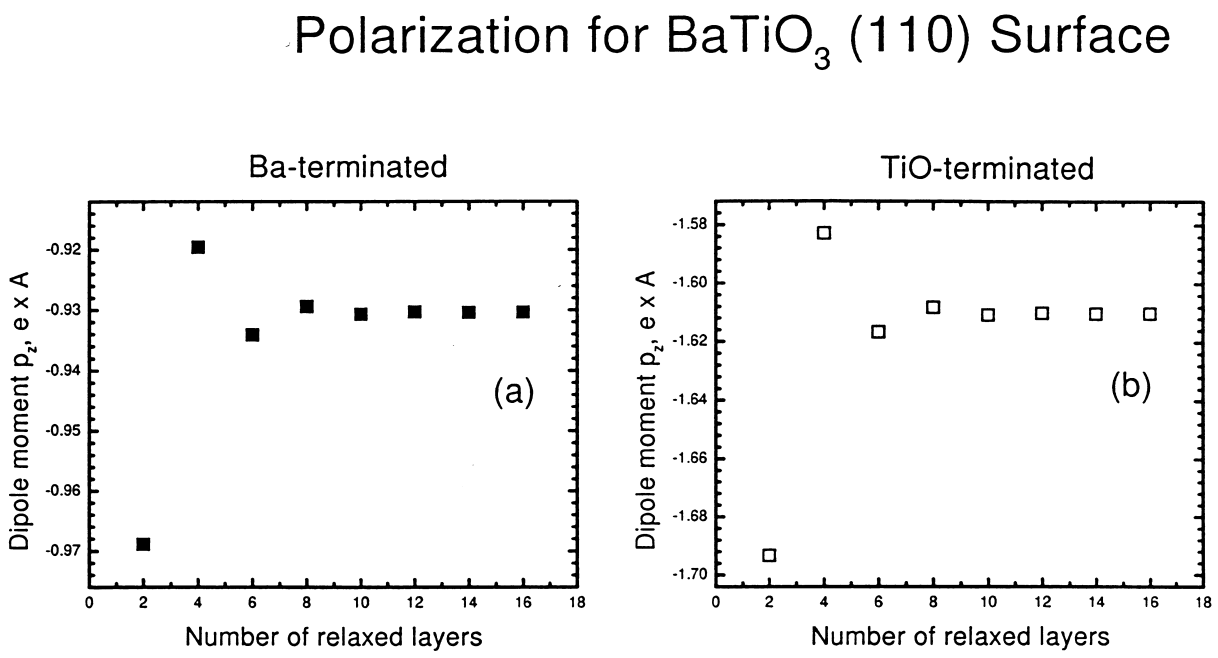

Fig. 9. Surface polarization of Ba- and TiO-terminated (110) surfaces.

only moderately ($\approx$4%) shifted outwards, but now the surface O ions tend to move inwards, so that they are displaced along the *z*-axis by as much as 11–14%. The surface O ions are also strongly polarized, and the relative core–shell separation is $\approx$4%. As a result, the first and second planes turn

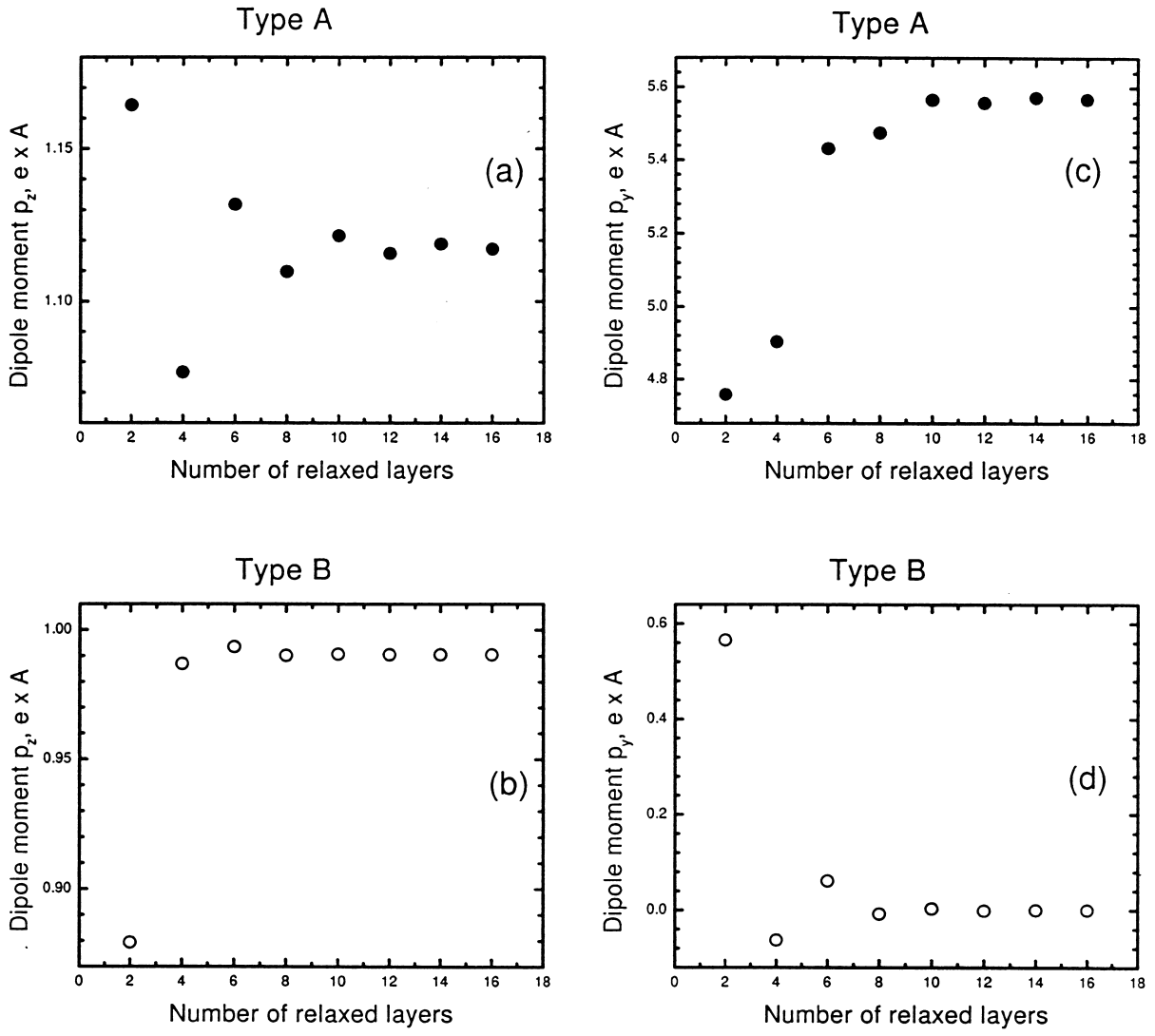

Fig. 10. Surface polarizations for the two types of O-terminated $BaTiO_3$ (110) (see Fig. 6b, c).

out to be strongly compressed, their separation is reduced by $\approx 12\%$, whereas the distance between the second and third planes increases by $\approx 9\%$ because of the strong O atom inward displacements in the third plane. Note that these O atoms are also strongly polarized.

Similarly to the (100) surface, the (110) surface-induced dipole moments oscillate as the number of relaxed near-surface layers increases from one to 10 (Figs. 9–12). For a larger number of relaxed layers, these oscillations practically vanish, and the dipole moment saturates. In other words, relax-

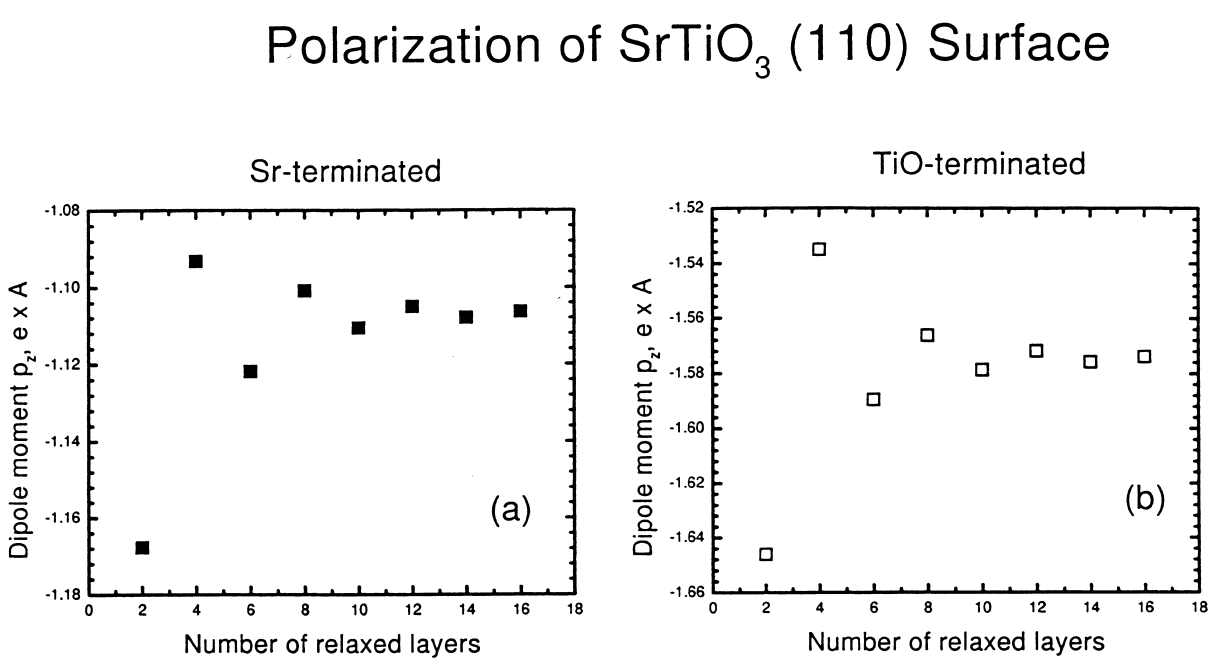

Fig. 11. Surface polarizations of Sr- and TiO-terminated $SrTiO_3$ (110) surfaces.

ation of (at least) 10 top layers is important for a correct description of the polarization for the (110) perovskite surfaces.

The values of the surface dipole moments perpendicular to the $BaTiO_3$ (110) (Fig. 9) saturate at the $-0.93\ e\cdot Å$ for Ba-terminated surfaces and $-1.61\ e\cdot Å$ for Ti-terminated surfaces. This is in sharp contrast with the results for the (100) surface (Figs. 4 and 5), for which we obtained dipole moments of $0.07\ e\cdot Å$ in the case of the Ba termination, and $-0.19\ e\cdot Å$ for the Ti-terminated surfaces. That is, the (110) surface dipole moments and surface polarizations, respectively, are much larger. In contrast, for the O-terminated $BaTiO_3$ in both initial configurations — asymmetric and symmetric — the dipole moments are positive and of the same order of magnitude as that for the Ba- and Ti terminations (Fig. 10a, b). It is important, however, to stress that in the asymmetric O configuration, *A* (Fig. 10c), we also observe the strong on-plane polarization, p_y, caused by the dipole moments much larger than those perpendicularly to the surface (Figs. 4 and 5). This is a manifestation of the ferroelectric reconstruction predicted for the first time for the (100) surface [26].

The perpendicular surface polarization of Sr- and Ti-terminated $SrTiO_3$ (Fig. 11) is quite similar to that for the $BaTiO_3$. However, dipole moments for the O-terminated asymmetric $SrTiO_3$ surface (Fig. 12c) reveal strong oscillations, even for 16 relaxed layers (similar to those observed above for the surface energy). This is caused by this surface

Table 8
Surface rumpling, *s*, and relative displacements of the three near-surface plane for the O- and Ti-terminated $SrTiO_3$ and $BaTiO_3$ (110) surfaces (as a percentage of the bulk lattice parameter) obtained for the symmetrical initial O position *B*, shown in Fig. 6a–c[a]

	O-terminated		Ti-terminated		
	Δd_{12}	Δd_{23}	*s*	Δd_{12}	Δd_{23}
$SrTiO_3$	2.36 (−11.83)	−2.73 (8.69)	14.47	−4.27	−3.86
$BaTiO_3$	3.34	−3.89	13.38	−5.27	−3.25

[a] Numbers in brackets correspond to the asymmetrical O position, *A*.

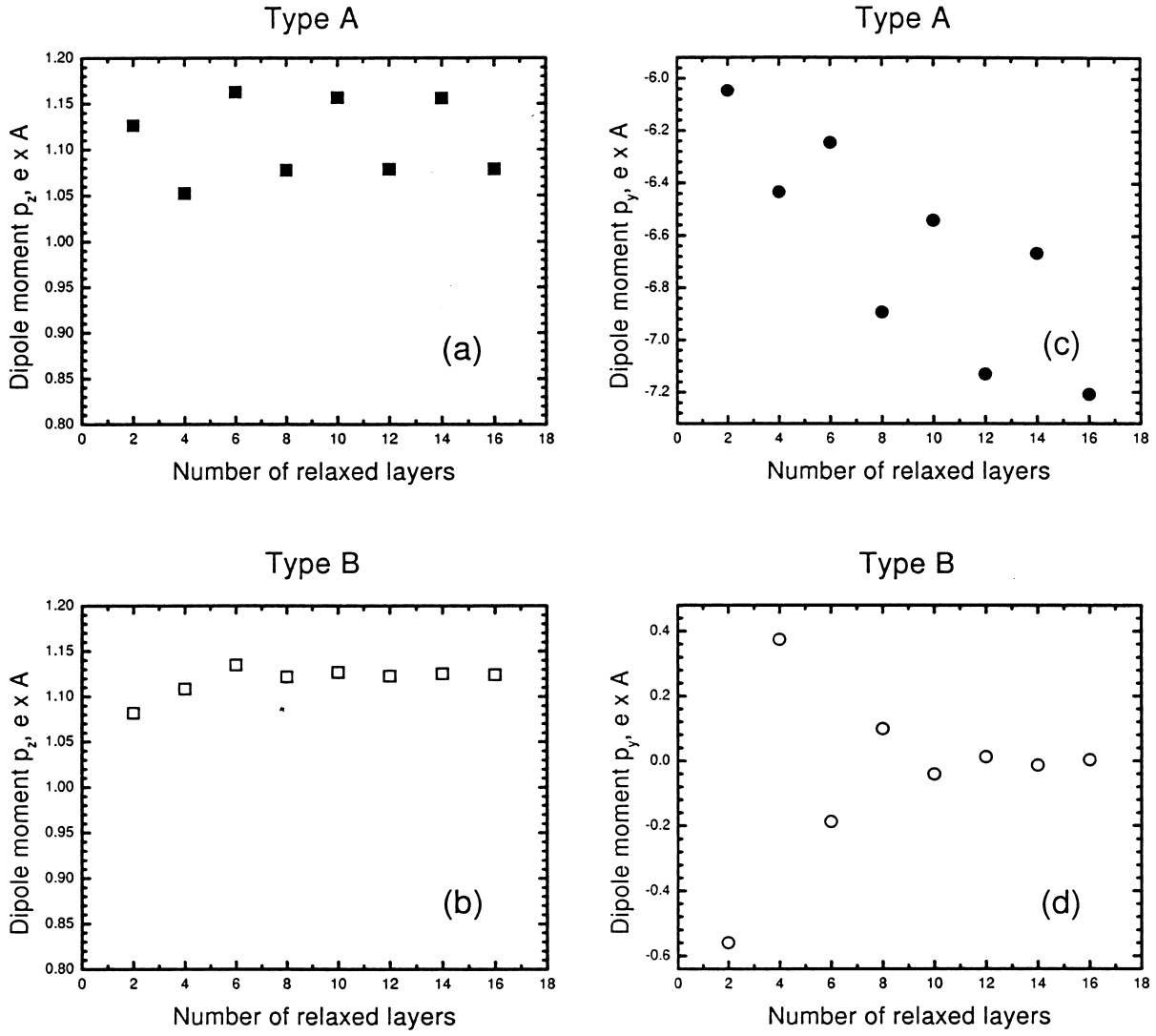

Fig. 12. Surface polarizations for the two types of O-terminated $SrTiO_3$ (110).

instability with respect to the ADF-type relaxation that is observed for $SrTiO_3$ at low temperatures. In contrast, p_y dipole moments for the symmetric O configuration saturate rapidly to zero (Fig. 12d).

4. Discussion and conclusion

A comparison of our semi-empirical SM results with ab-initio plane-wave pseudopotential calculations [12–14] and experimental low-energy

electron diffraction [7] studies of $SrTiO_3$ (001) surface clearly demonstrates the good agreement for the rumpling and the relative displacements between the second and third planes. We found that the properties of the $BaTiO_3$ and $SrTiO_3$ (100) surfaces were similar, in line with ab-initio calculations [12,13]. (Note that ab-initio calculations predict different properties of $PbTiO_3$ due to the higher covalency of the chemical bonding [14].)

Next, we found that the metal-terminated surface relaxations for $SrTiO_3$ and $BaTiO_3$ (110) surfaces are much larger than those for the (100). This is in line with observations for other oxides. For instance, an ab-initio Hartree–Fock study of O relaxation on MgO (110) surface estimates it to be as large as 7% of the interlayer distance [44], whereas the oxide surface relaxation reaches even 68% for the Al-terminated corundum surface [45]. Another important prediction of our calculations is the possibility of two quite different surface relaxations for the O-terminated surface obtained when we start with the two different surface O positions (symmetric and asymmetric). This indicates that the potential energy surface is quite complicated, and these two configurations are very likely separated by a considerable energy barrier. Note, however, that the symmetric O termination is energetically not favourable compared with the asymmetrical O termination. It is of great interest to check these results experimentally and by means of careful ab-initio calculations, which are in progress. It should be stressed here that the SM is also a promising tool for future studies of defect-induced processes in perovskites [20,21,37,46]. Another important problem to which the SM could contribute, is the strain in thin ferroelectric films caused by a substrate. It was shown recently [47] that even a small amount of stress could lead to the appearance of ferroelectricity in $SrTiO_3$.

The formation of dipole moments parallel and perpendicular to the surface in a cubic phase of perovskite could considerably affect the ferroelectric properties of thin films. Note that our calculations take into account the depolarization field.

Unfortunately, the only LEED study [32] available at the moment for $SrTiO_3$ (110) contains no quantitative estimates of the relative displacements of atoms from their positions in the ideal unrelaxed surface, which could be a good test of our theory.

Acknowledgements

This study was partly supported by the NATO Program for science senior visitors (through the Danish Research Agency grant No. 9800484 to E.A.K.). The authors are indebted to G. Borstel, F. Corá, N.E. Christensen, S. Dorfman, D. Fuks, J. Gavartin, R. de Souza and D. Vanderbilt for fruitful discussions.

References

[1] C. Noguera, Physics and Chemistry at Oxide Surfaces, Cambridge University Press, New York, 1996.
[2] V.E. Henrick, P.A. Cox, The Surface Science of Metal Oxides, Cambridge University Press, New York, 1994.
[3] M.E. Lines, A.M. Glass, Principles and Applications of Ferroelectrics and Related Materials, Clarendon Press, Oxford, 1977.
[4] O. Auciello, J.F. Scott, R. Ramesh, Phys. Today (1998) July, p. 22.
[5] Proc. Williamsburg Workshop on Ferroelectrics-99, J. Phys. Chem. Sol. 61 (2) (2000) Special Issue.
[6] W. Zhong, D. Vanderbilt, Phys. Rev. B 53 (1996) 5047.
[7] N. Bickel, G. Schmidt, K. Heinz, K. Müller, Phys. Rev. Lett. 62 (1989) 2009.
[8] T. Hikita, T. Hanada, M. Kudo, M. Kawai, Surf. Sci. 287–288 (1993) 377.
[9] M. Kudo, T. Hikita, T. Hanada, R. Sekine, M. Kawai, Surf. Interf. Anal. 22 (1994) 412.
[10] A. Ikeda, T. Nishimura, T. Morishita, Y. Kido, Surf. Sci. 433–435 (1999) 520.
[11] T. Nishimura, A. Ikeda, H. Namba, T. Morishita, Y. Kido, Surf. Sci. 421 (1999) 273.
[12] J. Padilla, D. Vanderbilt, Surf. Sci. 418 (1998) 64.
[13] J. Padilla, D. Vanderbilt, Phys. Rev. B 56 (1997) 1625.
[14] B. Meyer, J. Padilla, D. Vanderbilt, Faraday Discuss. 114 (1999) 395.
[15] F. Corá, C.R.A. Catlow, Faraday Discuss. 114 (1999) 421.
[16] L. Fu, E. Yachenko, L. Resca, R. Resta, Phys. Rev. B 60 (1999) 2697.
[17] K. Ishikawa, T. Uemori, Phys. Rev. B 60 (11) (1999) 841.
[18] C.R.A. Catlow, W.C. Mackrodt (Eds.), Computer Simulation of Solids Lecture Notes in Physics, Vol. 166, Springer, Berlin, 1982.
[19] H.-J. Donnerberg, Atomic Simulation of Electrooptic and Magnetooptic Oxide Materials, Springer Tracts in Modern Physics, Vol. 151, Springer, Berlin, 1999.
[20] G.V. Lewis, C.R.A. Catlow, J. Phys. C 18 (1985) 1149.

[21] G.V. Lewis, C.R.A. Catlow, J. Phys. Chem. Solids 47 (1986) 89.
[22] M.J. Akhtar, Z.N. Akhtar, R.A. Jackson, C.R.A. Catlow, J. Am. Ceram. Soc. 78 (1995) 421.
[23] M. Cherry, M.S. Islam, J.D. Gale, C.R.A. Catlow, J. Phys. Chem. 99 (1995) 14614.
[24] M. Cherry, M.S. Islam, J.D. Gale, C.R.A. Catlow, J. Solid State Chem. 118 (1995) 125.
[25] H. Donnerberg, M. Exner, Phys. Rev. B 49 (1994) 3746.
[26] V. Ravikumar, D. Wolf, V.P. Dravid, Phys. Rev. Lett. 74 (1995) 960.
[27] J. Prade, U. Schröder, W. Kress, F.W. de Kulkarni, J. Phys.: Condens. Matter 5 (1993) 1.
[28] H. Bando, Y. Aiura, Y. Haruyama, T. Shimizu, Y. Nishihara, J. Vac. Sci. Technol. B 13 (1995) 1150.
[29] K. Szot, W. Speier, Phys. Rev. B 60 (1999) 5909.
[30] J. Brunen, J. Zegenhagen, Surf. Sci. 389 (1997) 349.
[31] Q.D. Jiang, J. Zegenhagen, Surf. Sci. 425 (1999) 343.
[32] J. Zegenhagen, T. Haage, Q.D. Jiang, Appl. Phys. A 67 (1998) 711.
[33] R. Souda, Phys. Rev. B 60 (1999) 6068.
[34] Y. Adachi, S. Kohiki, K. Wagatsuma, M. Oku, J. Appl. Phys. 84 (1998) 2123.
[35] A. Pojani, F. Finocchi, C. Noguera, Surf. Sci. 442 (1999) 179.
[36] W.G. Stirling, J. Phys. C: Solid State Phys. 5 (1972) 2711.
[37] J. Crawford, P.W.M. Jacobs, J. Solid State Chem. 144 (1999) 423.
[38] D.H. Gay, A.L. Rohl, J. Chem. Soc. Faraday Trans. 91 (1995) 925.
[39] E. Heifets, S. Dorfman, D. Fuks, E.A. Kotomin, Thin Solid Films 296 (1997) 76.
[40] E. Heifets, S. Dorfman, D. Fuks, E.A. Kotomin, A. Gordon, J. Phys.: Condens. Matter 10 (1998) L347.
[41] S. Dorfman, D. Fuks, E. Kotomin, Thin Solid Films 318 (1998) 65.
[42] P.W. Tasker, J. Phys. C: Solid State Phys. 12 (1979) 4977.
[43] E. Heifets, E.A. Kotomin, Thin Solid Films 358 (2000) 1.
[44] M. Causá, E.A. Kotomin, C. Pisani, J. Phys. C: Solid State Phys. 20 (1987) 4383.
[45] V.E. Puchin, J.D. Gale, A.L. Shluger, E.A. Kotomin, J. Günster, M. Brause, V. Kempter, Surf. Sci. 370 (1997) 190.
[46] R.A. de Souza, M.S. Islam, E. Ivers-Tiffee, J. Mater. Chem. 9 (1999) 1621.
[47] N.A. Pertsev, A.K. Tagantsev, N. Setter, Phys. Rev. B 61 (2000) 825.